

# EIS evaluation of protective performance and surface characterization of epoxy coating with aluminum nanoparticles after wet and dry corrosion test

A. Madhankumar · S. Nagarajan · N. Rajendran ·  
T. Nishimura

Received: 13 May 2011 / Revised: 21 November 2011 / Accepted: 13 December 2011 / Published online: 25 December 2011  
© Springer-Verlag 2011

**Abstract** The effect of addition of aluminum (Al) nanoparticles to epoxy coating on the ability to protect the carbon steel was studied by electrochemical impedance spectroscopy and focused ion beam-transmission electron microscopy. The EIS was conducted in 0.1 M NaCl solution after wet/dry cyclic corrosion test. The addition of Al nanoparticles increased the film resistance ( $R_f$ ) and the charge transfer resistance ( $R_{ct}$ ) of epoxy-coated steel. The surface analysis showed that uniform and fine Al-Fe complex oxide layers were formed acting as barrier layers that enhanced the corrosion protection of the epoxy-coated steel. It has been concluded that the Al nanoparticles had a beneficial role in improving the corrosion resistance of the epoxy-coated steel.

**Keywords** Coatings · Al nanoparticles · Corrosion · EIS · FIB-TEM

## Introduction

A general and inexpensive approach to enhance corrosion resistance of carbon steel (CS) is to apply protective coatings on their surface [1, 2]. Organic coatings have been used to protect structural materials against corrosion. However,

their poor durability has been well documented [3]. To overcome this cumbersome, inhibitive elements have been introduced into organic coatings. Commonly, zinc (Zn) rich coatings have been used owing to their ability to act as a sacrificial coating to protect steel against corrosion [4–9]. Nevertheless, the available resources of Zn in the earth are decreasing markedly. Thus, as an alternative to Zn, Al coatings have been used in recent years to protect the structural materials in corrosive environment [10].

Sometimes, Al forms a passive film on the surface, it does not show the sacrificing effect against steel. On the other hand, nanomaterials and nanoparticles have been widely developed for various applications [11–14]. By reducing the size of particles to the nano-level, the activity of the surface is to be significantly improved. Moreover, the incorporation of Al nanoparticles into the organic coatings helps to develop environmental friendly coatings. Although Al nanoparticles have been used for advanced energetic materials [15], few studies have focused on their anticorrosion properties resulting from the addition of nano Al to the coatings [16]. Shi et al. [17] have reported the role of nanoparticles viz., SiO<sub>2</sub>, Zn, Fe<sub>2</sub>O<sub>3</sub>, and holloysite clay introduced into epoxy coatings on steel in NaCl solution. Moreover, epoxy coatings containing nanoparticles are expected to enhance the barrier properties for corrosion protection and reduce blister or delamination in the coating [18, 19].

In this study, we utilized Al nanoparticles in epoxy coatings to achieve the sacrificing effect against corrosion of steel in 0.1 M NaCl solution under a wet/dry cyclic condition. In order to investigate the effect of Al nanoparticles, the electrochemical behavior of the coated steel was investigated by the electrochemical impedance spectroscopy (EIS), and the corrosion products of the coated steel were examined by field emission-scanning electron microscopy

A. Madhankumar · S. Nagarajan · T. Nishimura (✉)  
Research centre for strategic materials,  
National Institute for Material Science(NIMS),  
1-2-1 Sengen,  
Tsukuba, Ibaraki 305-0047, Japan  
e-mail: nishimura.toshiyasu@nims.go.jp

A. Madhankumar · N. Rajendran  
Department of Chemistry, Anna University,  
Chennai-25, India

(FE-SEM) and focused ion beam-transmission electron microscopy (FIB-TEM) after wet/dry cyclic corrosion test.

## Experimental procedure

### Preparation of specimens

The chemical composition of the CS specimens in mass% was JIS-SM, 0.1C–0.3Si–0.7Mn–0.01P–0.003S–0.03Al–0.003N–0.002O–Fe. The specimen, with a surface area of 25 cm<sup>2</sup>, was polished with silicon carbide (SiC) papers up to 1,200 grit. After polishing, the sample surface was rinsed with distilled water and acetone before coating.

### Preparation of coatings

The epoxy resin used in this investigation was commercially available fast drying type. The liquid epoxy resin was a blend of multifunctional low molecular weight diluents and the diglycedal ether of bis-phenol-A, whereas the curing agent was based on the aliphatic amines. The weight ratio of the epoxy resin to the curing agent was 2:1. The commercially available Al nanoparticles of size ranging from 300 to 500 nm were used. The Al nanoparticles of 40 mass% were added to the epoxy resin and were coated using draw-down bar at constant speed and then kept at room temperature for 24 h. This led to the formation of uniform coating with thickness of about 40 μm. The epoxy coatings without Al nanoparticles were also applied by the same procedure.

### Electrochemical measurement

The EIS measurements were performed in a conventional three-electrode cell, using a coated steel specimen as the working electrode and a saturated calomel electrode (SCE) as the reference electrode. A frequency response analyzer (FRA) was used for EIS measurements using amplitude of 10 mV over a frequency range from 40 kHz to 1 mHz. The specimen area of the steel was 25 cm<sup>2</sup> and other surfaces were sealed. The EIS measurements were conducted after wet/dry cyclic condition (12 h immersion in 0.1 M NaCl solution and 12 h in dry condition) for 15 days. All the measurements were carried out in open circuit potential (OCP) at room temperature (25°C) in 0.1 M NaCl solution. The EIS experimental data were analyzed using curve fittings by Zsindemo software.

### Surface characterization

The surface state of the corrosion product on the coated steel was observed by FE-SEM analysis. After cyclic corrosion test, the coated steel was cast in resin. The resin was cured

and the disc was cross-sectioned. The exposed cross-section was then polished using emery paper, followed by diamond paste. Carbon was then evaporated on the specimen in order to compensate for charging effects. A cross section of the rusted steel was examined using FE-SEM at an acceleration voltage of 20 kV and irradiation current of 10 μA. The concentration of Al and Fe in the rust was measured by EDAX (energy dispersive X-ray) analysis.

TEM observation was performed with EDAX analysis. The rust was cut from the inner rust by FIB (focused ion beam). The line profile analysis was carried out in order to identify the concentration of Fe and Al in the rust.

## Results and discussion

### EIS behavior of coated steel in cyclic corrosion test

Figures 1 and 2 show the EIS results for the steel coated by epoxy without and with 40% Al nanoparticles, respectively, after wet/dry corrosion test for 15 days. The EIS spectrum of the coated steels shows the two capacitances and two resistances. In the high-frequency region, EIS spectra are thought to exhibit the coating behaviors, and in the low-frequency region, the spectra corresponded to corrosion reaction occurring on the metal under the coating [20]. Thus, the resistance in the high-frequency region showed the resistance of the film

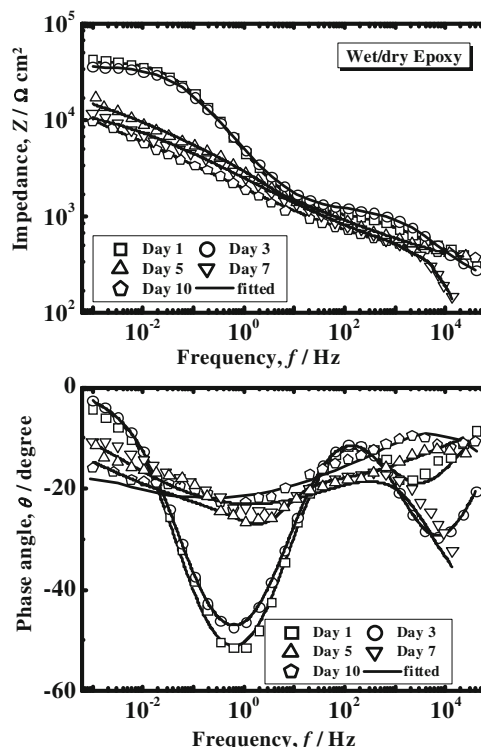


**Fig. 1** EIS results of steel coated by epoxy without 40% Al after wet/dry cycles test in 0.1 M NaCl solution for different durations

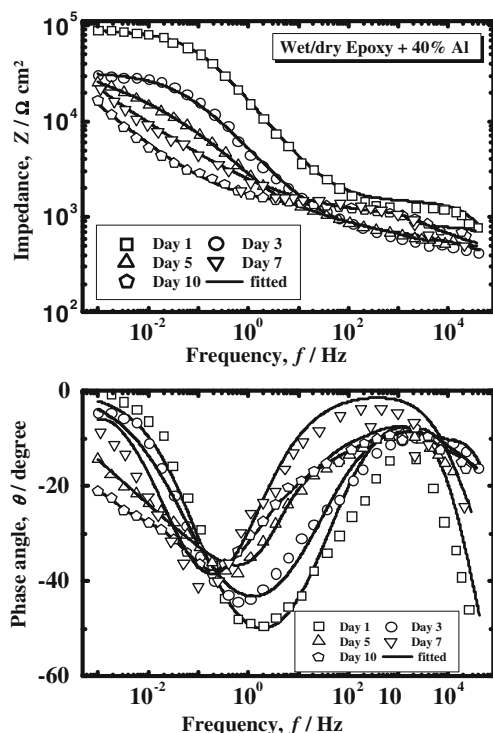
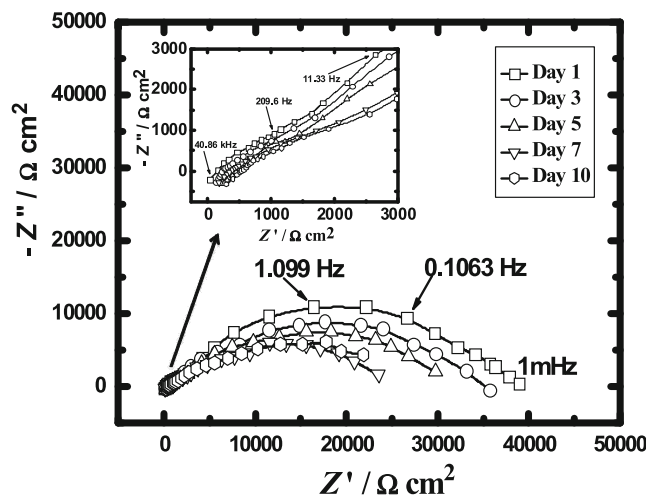


**Fig. 2** EIS results of steel coated by epoxy with 40% Al after wet/dry cycles test in 0.1 M NaCl solution for different durations

( $R_f$ ) of 1–15  $k\Omega\text{ cm}^2$ , while the resistance in the low-frequency region showed the charge transfer resistance ( $R_{ct}$ ) of 5.5–70  $k\Omega\text{ cm}^2$ . The EIS spectra suggest the presence of two capacitances. As the capacitance at high frequency showed a lower value of  $10^{-10}$ – $10^{-6}\text{ F cm}^{-2}$ , it was thought to be the film capacitance. As the capacitance at lower frequency showed a higher value of  $10^{-5}$ – $10^{-2}\text{ F cm}^{-2}$ , which was attributed to the double layer capacitance [21].

Figures 3 and 4 show the Nyquist plots for the steel coated by epoxy without and with 40% Al nanoparticles, respectively. Nyquist plots of coated steels were clearly showed the two capacitive loops in the high-frequency and low-frequency regions, attributed to the resistance and capacitance of the coating and steel–electrolyte interface, respectively. These EIS curves represented the electrochemical process with two time constants, which were well separated.

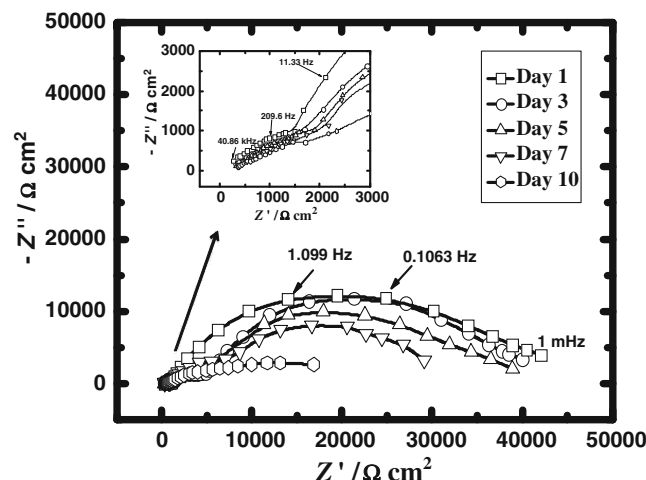
In this study, all EIS data could be fitted using the equivalent circuit model shown in Fig. 5. Thus, the corrosion of the coated steel was estimated by the equivalent circuit composing the solution resistance ( $R_{sol}$ ), film capacitance ( $C_f$ ), double layer capacitance ( $C_{dl}$ ), film resistance ( $R_f$ ), and charge transfer resistance ( $R_{ct}$ ). The CPE (constant phase element) was used to replace the double layer capacitance ( $C_{dl}$ ) because of the deviation of  $C_{dl}$  from its ideal capacitive behavior. The CPE is defined by the following relation  $Z=Y_0^{-1}(j\omega)^{-n}$ , where  $Z$  is the impedance of the CPE,  $j$  is the imaginary number ( $j^2=-1$ ),  $\omega$  is the angular frequency (radians per second ( $\text{rad s}^{-1}$ )),  $Y_0$  and  $n$  are the frequency independent parameters.



**Fig. 3** Nyquist plot of steel coated by epoxy without 40% Al after wet/dry cycles test in 0.1 M NaCl solution for different durations

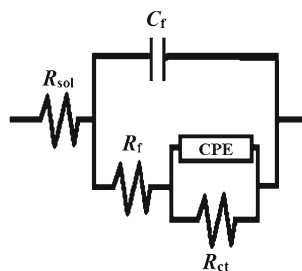
The  $n$  value ranging from 0 to 1 depends on the surface roughness. For the perfect surface, the value of  $n$  is 1 and the impedance of CPE is that of pure capacitor [22]. The fitted curves are in good agreement with the actual results.

Figure 6a shows the change in  $R_{ct}$  with time obtained by curve fitting. In the case of steel coated by epoxy without nanoparticles, the  $R_{ct}$  value was found to be 5.5  $k\Omega\text{ cm}^2$  after 15 days. However,  $R_{ct}$  of steel coated by epoxy with Al40% nanoparticles exhibited a higher value of 20  $k\Omega\text{ cm}^2$  and become constant after 8 days. For instance, the  $R_{ct}$  value at the 15th day was approximately three times higher (around 17  $k\Omega\text{ cm}^2$ ) than coated steel by epoxy without nanoparticles. It was clearly observed that the steel coated by epoxy with Al 40% nanoparticles showed significantly high resistance compared to steel coated by epoxy without Al nanoparticles during the wet/dry cycles. This could be explained based on the expression,  $R = \rho \times l$ , where  $R$  is the resistance,



**Fig. 4** Nyquist plot of steel coated by epoxy with 40% Al after wet/dry cycles test in 0.1 M NaCl solution for different durations

**Fig. 5** Equivalent circuit diagram for steel coated by epoxy with and without 40% Al after wet/dry cycles test in 0.1 M NaCl solution for different durations

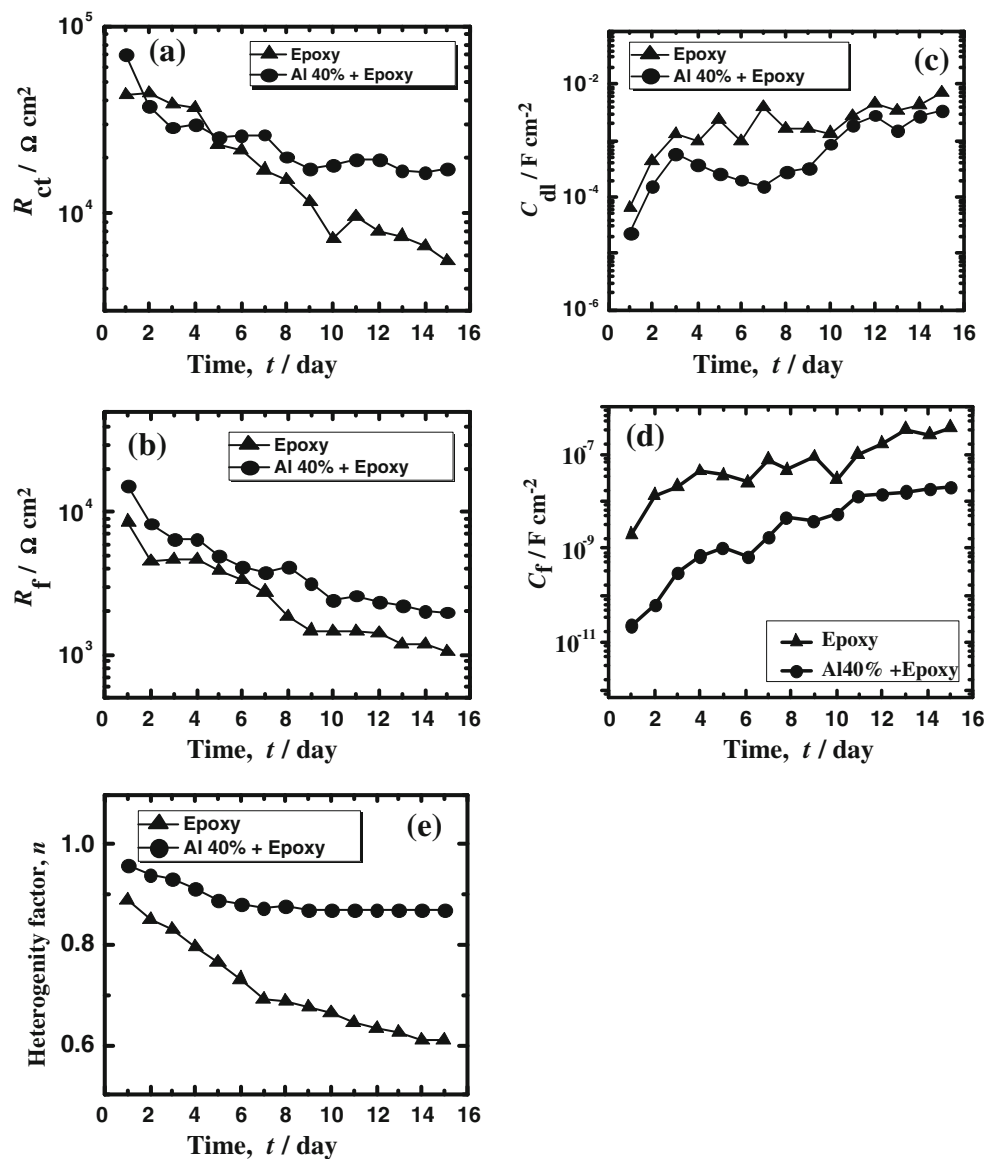


$\rho$  is the specific resistivity ( $\Omega \text{ cm}^{-1}$ ) of the coated steel and  $l$  is the thickness (centimeter) of the coatings [23]. The thickness of the epoxy coatings with and without Al nanoparticles were 40  $\mu\text{m}$ , since the same draw-down rod were used. It can be seen that the steel coated by epoxy with Al nanoparticles had a higher resistance as a result of high

specific resistivity compared to epoxy without Al nanoparticles. Hence, it was confirmed that the addition of Al nanoparticles increased the resistance of the coated steel.

Figure 6b shows the change in  $R_f$  with time obtained by curve fitting. The  $R_f$  value is attributed with ionic transport through the coating. The steel coated by epoxy without nanoparticles exhibited a rapid decrease in  $R_f$  during the exposure time, then, it remained constant at a low value (around 1.4  $\text{k}\Omega \text{ cm}^2$ ) after 10 days of exposure. This result indicated a rapid loss of the barrier properties of the film [24]. The decrease of  $R_f$  during the first few days of exposure was attributed to the penetration of the electrolyte through the coating. However, for the epoxy coating with Al nanoparticles, the  $R_f$  decreased slowly during the exposure time, and then remained constant at a higher value of 3.1  $\text{k}\Omega \text{ cm}^2$  compared to pure epoxy-coated steel. The

**Fig. 6** Equivalent circuit parameters **a**  $R_{ct}$ , **b**  $R_f$ , **c**  $C_{dl}$ , **d**  $C_f$ , and **e**  $n$  values for steel coated by epoxy with and without 40% Al in 0.1 M NaCl solution for different durations



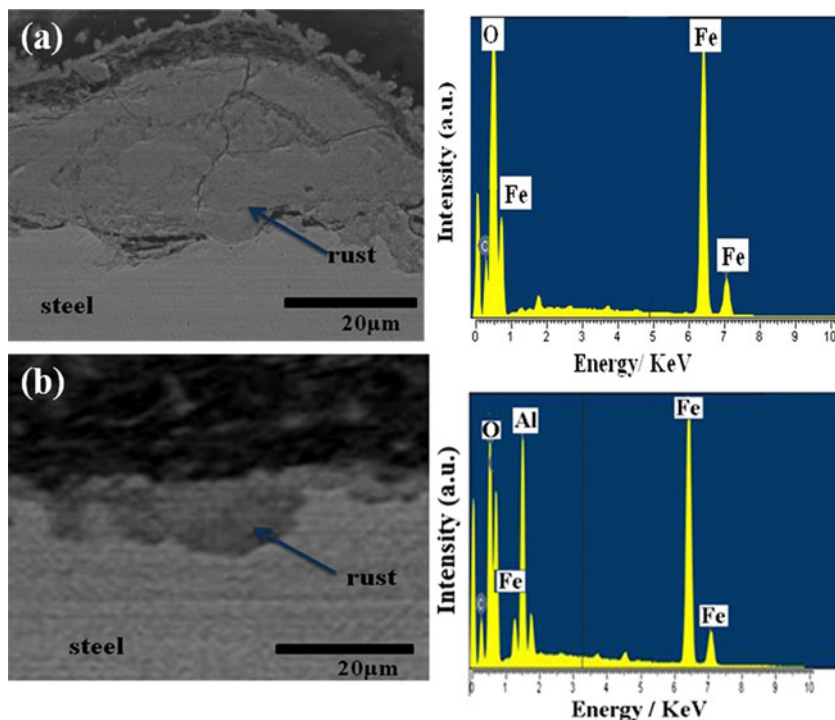
increase in value of  $R_f$  by the addition of Al nanoparticles in epoxy exhibited the enhancement of barrier properties of the coating.

The capacitance was represented by the following expression,  $C = \epsilon_0 \epsilon_r A/d$ , where  $\epsilon_0$  is the permittivity in vacuum,  $\epsilon_r$  is the relative permittivity of epoxy coating,  $A$  is the area of the coated surface, and  $d$  is the thickness of the epoxy coating [25]. In general, the relative dielectric constant of an epoxy coating is at least one order of magnitude lower than that of water, the permeation of water through the coating induces an increase of the capacitance value due to the increase of  $\epsilon_r$ , which can be accurately determined with EIS measurements [26]. Figure 6c shows the change in double layer capacitance ( $C_{dl}$ ) values with time by curve fitting. The  $C_{dl}$  values of steels coated by epoxy with and without Al nanoparticles were found to be low initially, in the order of  $10^{-5}$  F cm<sup>-2</sup>, then increased gradually with immersion time. This behavior could be attributed to water absorption. After a long time, the  $C_{dl}$  values for the epoxy with Al nanoparticles showed a lower value compared to that of epoxy without nanoparticles. In case of the steel coated by epoxy without nanoparticles, it had many micro-defects (pores) through which penetration of water and Cl<sup>-</sup> ions took place and reached the metal surface. This could lead to the beginning of the corrosion process on the metallic surface. However, the steel coated by epoxy with Al 40%, the microdefects were covered by corrosion product with Al nanoparticles that suppress the penetration of Cl<sup>-</sup> ions, which reduces the value of  $C_{dl}$ .

Figure 6d displays the change in film capacitance ( $C_f$ ) values with time by curve fitting. The value of  $C_f$  could be used to determine the water uptake by the organic coatings. An increase in the water uptake generally indicates loss of the protective properties of the coating and it reduced the adhesion/cohesion of the coating. The volume of fraction of water uptake can be calculated from the following expression, percent water uptake =  $[100 \log (C_f(t)/C_f(0))/\log 80]$  [27], where  $C_f(t)$  is the coating capacitance in time  $t$ ,  $C_f(0)$  is the coating capacitance at  $t=0$  and 80 corresponds to the dielectric constant of water. It is important to note that the epoxy with Al nanoparticles exhibit lowest water uptake which was found to be 9.3%, whereas the epoxy without Al nanoparticles was found to be 28.4%. Hence, it was concluded that the addition of Al nanoparticles prevent the penetration of water through epoxy coating which in turn reduce the corrosion under the metal/coating interface.

Figure 6e shows the change in values of  $n$  (heterogeneity factor) with time by curve fitting. The value of  $n$  is attributed to heterogeneity of metal surface due to corrosion process in metal coating interface [28, 29]. In the case of steel coated by epoxy without nanoparticles, the value of  $n$  was rapidly decreased during immersion time and found to be 0.61 after 15 days. However, the steel coated by epoxy with Al40% nanoparticles exhibited a higher value of 0.96 during immersion time and then remained constant at a higher value of 0.87 after 8 days. For instance,  $n$  value at the 15th day was significantly higher (around 0.87) than coated steel by epoxy without nanoparticles. This behavior indicated that the corrosion

**Fig. 7** a SEM image with EDAX results of coated steel by epoxy without 40% Al and b SEM image with EDAX results of coated steel by epoxy with 40% Al after wet/dry cycles test in 0.1 M NaCl solution



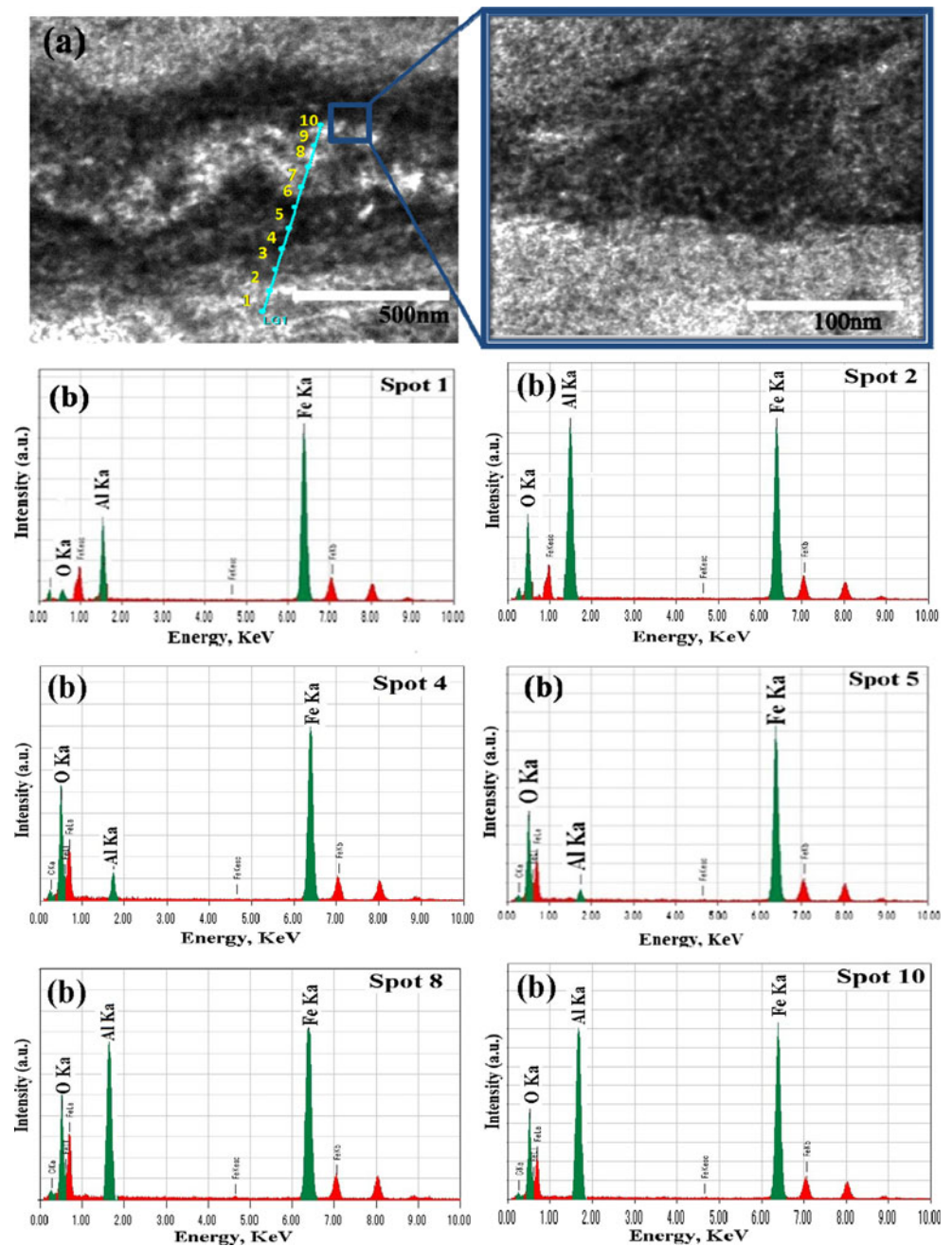
process occurred during the initial exposure time, then formed corrosion product with Al nanoparticles reduced the further corrosion process in metal coating interface.

#### Surface characterization of coated steel after wet/dry test

In order to identify the corrosion preventing mechanism, the surface of coated steel was analyzed after 15 days of wet/dry cyclic corrosion test using SEM. Figure 7a shows the cross-section of SEM and EDAX results for the steel coated by epoxy without Al nanoparticles. The higher amount of Fe and

oxygen in the rust from EDAX analysis indicated that the corrosion occurs strongly under metal/coating interface. Figure 7b shows the cross-section of SEM and EDAX results for steel coated by epoxy with Al nanoparticles. As Fe and Al showed higher concentration, Al and Fe were enriched in the rust. It is also clearly indicated that the Al nanoparticles added sample showed enrichment of Al and Fe, whereas the sample without Al nanoparticles exhibited more amount of rust with high intensity of Oxygen and Fe. Moreover, Al was presumed to form a complex oxide with iron [30] since complex oxides containing Al were identified with Fe by EDAX. This result

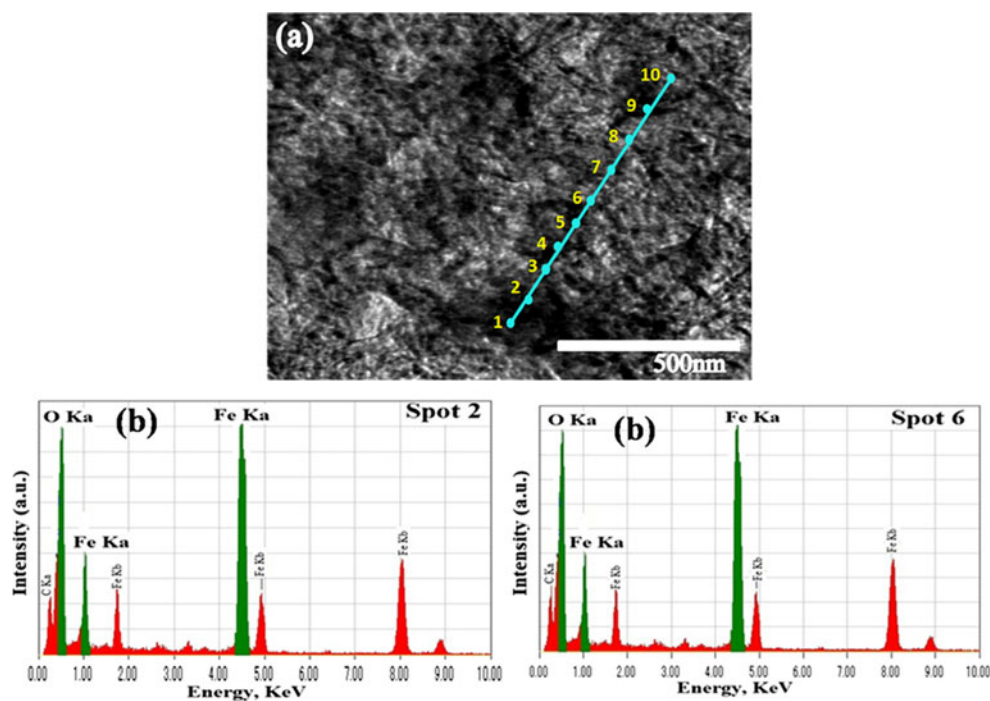
**Fig. 8** a Bright field image and b EDAX results by FIB-TEM analysis for the rust on the steel coated by epoxy with 40% Al after wet/dry cycle test in 0.1 M NaCl solution



implies that the complex oxides were formed during the cyclic corrosion test which could enhance the barrier penetration properties of the epoxy coatings.

In order to investigate the nanostructure of the rust of coated steel by epoxy with and without Al nanoparticles, TEM analysis was carried out, and the micrographs depicted the spot position analysis. The inner rust was cut by FIB (focused ion beam). Figure 8 shows the TEM and EDAX spot analysis results of rust of coated steel by epoxy with Al nanoparticles. As Al is a light metal, it is shown as the white color in the bright field image of the TEM [31]. Thus, it was possible to select the rust containing Al and Fe by EDAX analysis. Figure 8b shows the EDAX analysis around the inner rust. It is observed that the spot 1 and 2 of the inner rust showed a sharp peak for Al. However, spots 5 and 6 showed small peaks for Al and large peaks for Fe. In addition, spots 8 and 10 also showed sharp peaks for Al. Thus, there were Al-rich and poor positions in the rust. Figure 9 shows the TEM and EDAX spot analysis results of rust in the coated steel by epoxy without Al nanoparticles. It is observed that both spot 2 and 6 exhibits the sharp peaks for Fe and Oxygen. In the case of rust with Al nanoparticles, it showed lower amount of Fe and oxygen in all the spots compared to that of rust without nanoparticles. This also clearly indicates an enrichment of Al and also a decrease in the mass percent of Fe in the white filled areas. Actually, these white particles were nano-level size and made up the layered structure that was enriched by oxides with Al and Fe. In other words, nanoscale complex oxides containing Al and Fe were formed in the rust of steel, and these oxide layers increased the corrosion resistance of this steel.

**Fig. 9** a Bright field image and b EDAX results by FIB-TEM analysis for the rust on the steel coated by epoxy without 40% Al after wet/dry cycle test in 0.1 M NaCl solution



Corrosion mechanism of epoxy with Al nanoparticles coated steel

The incorporation of Al nanoparticles into the epoxy coating increased the  $R_{ct}$  and  $R_f$  after wet/dry test. The enhancement of these values observed for steel coated with Al nanoparticles could be explained by two possible mechanisms.

First, the presence of Al nanoparticles in coating matrix reduce the possibility of electrolyte penetration that leads to a decrease of effective area for charge transfer reaction of anodic reaction on steel surface. It has been already reported that the rust of carbon steel containing Al was a cation permeability which prevents the penetration of  $Cl^-$  ions from the electrolyte [32], whereas the rust of carbon steel without Al was an anion permeability which allowed the passage of  $Cl^-$  ions leading to corrosion under metal/coating interface. In addition, Al nanoparticles reduce the micro-defects in the coating film by making the corrosion products and covering the pores (microdefects) of the epoxy coating. This behavior could impede the penetration path of chloride ions, leading to improved barrier performance.

Another possible mechanism is that the formation of the nanoscale complex oxides of Al and Fe suppress the anodic reaction of steels. In the actual results,  $R_{ct}$  was dramatically increased by the addition of Al nanoparticles. On other hand,  $R_f$  was to some extent increased. Thus, the effect of Al nanoparticles is considered significant in forming corrosion products and suppressing anodic reaction.

In both cases, the barrier effect of coating could be increased. The detail mechanism is thought to be the following model. During the cyclic corrosion test, the

corrosion reaction took place in a wet condition during cyclic corrosion test and Al nanoparticles dissolved from the epoxy-coated steel, which exists in wet surface in its ionic form. In the beginning of the following dry cycles, a thin wet surface still could exist. The top of the wet surface thought to be rich in Al ions, then, because of the solubility, started to make complex oxides with Fe in the dry process. It was assumed that the oxides containing Al were fine and of low solubility and that the oxides without Al were large and of high solubility. In addition, it has been already reported that the solubility of iron oxides tends to decrease with increasing the Al addition [33, 34]. Thus, oxides containing Al precipitated at the bottom of the wet surface, and oxides without Al precipitated at the top of the wet surface. In the dry process, these oxides made Al-rich and Al-poor regions in the corrosion products. As a result, the Al-enriched layer was formed in one dry process. During wet/dry test, these layers were increasing and made large corrosion products. This is a reasonable explanation because Fe and Al complex oxide was formed in the rust as measured by FIB-TEM analysis. Because of this, it was concluded that Al nanoparticles had a beneficial effect on corrosion resistance of coated steel by making corrosion products in wet/dry cyclic test.

## Conclusions

Using EIS and FIB-TEM, the effect of Al nanoparticles on the corrosion resistance of epoxy-coated steel has been evaluated after wet/dry corrosion test. The following main results were obtained. From EIS analysis, it was observed that the  $R_f$  and  $R_{ct}$  of steel coated by epoxy with 40% nanoparticle was higher than epoxy-coated steel in the wet/dry corrosion test. This behavior showed that the addition of Al nanoparticle resulted in high corrosion resistance in wet/dry test. FIB-TEM analysis confirmed that the nano-complex oxides containing Al and Fe were enriched in the rust of the coated steel. It can be concluded that Al nanoparticles had a beneficial effect on the enhancement of corrosion resistance of coated steel in wet/dry cyclic test.

## References

1. Mayne JEO (1994) The mechanism of protective action of paints. In: Shreir LL, Jarman RA, Burstein GT (eds) Corrosion. Butterworth Heinemann, Oxford, pp 22–32
2. Hare C (2000) Corrosion control of steel by organic coatings. In: Review RW (ed) Uhlig's corrosion handbook. John Wiley & Sons, New York, pp 1023–1038
3. Greenfield D, Scantlebury D (2000) The protective action of organic coatings on steel: a review. *J Corros Sci Eng* 3:5
4. Ross TK, Wolstenholme J (1977) Anti corrosion properties of zinc dust paints. *Corros Sci* 17:341–351
5. Pereira D, Scantlebury J, Ferreira M, Almeida M (1990) The application of electrochemical measurements to the study and behavior of zinc rich coatings. *Corros Sci* 30:1135–1147
6. Felix S, Barajas R, Bastidas JM, Morcillo M, Feliu S (1993) In: Scully JR, Silverman DC, Kendig M (eds) Study of protections mechanism of zinc rich paints by electrochemical impedance spectroscopy, electrochemical impedance spectroscopy, ASTM STP 1188. Amer Soc Testing and Materials (ASTM), Philadelphia, pp 438–449
7. Gervasi CA, Di Sarli AR, Cavalcanti E, Ferraz O, Bucharsky EC, Real SG, Vilche JR (1994) The corrosion protection of steel in sea water using zinc rich alkyd paints. An assessment of the pigment content effect by EIS. *Corros Sci* 36:1963–1972
8. Abreu CM, Izquierdo M, Merino P, Nóvoa XR, Pérez C (1999) A new approach to the determination of the cathodic protection period in zinc-rich paints. *Corrosion* 55:1173–1181
9. Shreepathi S, Balaji P, Malik BP (2010) Electrochemical impedance spectroscopy investigations of epoxy zinc rich coatings: role of Zn content on corrosion protection mechanism. *Electrochim Acta* 55:5129–5134
10. González S, Mirza Rosca IC, Souto RM (2001) Investigation of the corrosion resistance characteristics of pigments in alkyd coatings on steel. *Prog Org Coat* 43:282–285
11. Arango AC, Carter SA, Brock PJ (1999) Charge transfer in photo-voltaics consisting of interpenetrating networks of conjugated polymer and TiO<sub>2</sub> nanoparticles. *Appl Phys Lett* 74:1698–1700
12. Voevodin N, Balbyshev VN, Khobaib M, Donley MS (2003) Nanostructured coatings approach for corrosion protection. *Prog Org Coat* 47:416–423
13. Schnitzler Danielle C, Zarbin Aldo JG (2004) Organic/inorganic hybrid materials formed from TiO<sub>2</sub> nanoparticles and polyaniline. *J Braz Chem Soc* 15:378–384
14. Ghicov A, Tsuchiya H, Macak J, Schmuki P (2005) Titanium oxide nanotubes prepared in phosphate electrolytes. *Electrochem Comm* 7:505–509
15. Mukherjee D, Rai A, Zachariah MR (2006) Quantitative laser-induced breakdown spectroscopy for aerosols via internal calibration: application to the oxidative coating of aluminum nanoparticles. *J Aero Sci* 37:677–695
16. Xue L, Xu L, Li Q (2007) Effect of nano Al pigment on the anticorrosive performance of waterborne epoxy coatings. *J Mater Sci Technol* 23:563–567
17. Shi X, Nguyen TA, Suo Z, Liu Y, Avci R (2009) Effect of nanoparticles on the anticorrosion and mechanical properties of epoxy coating. *Surf Coat Technol* 204:237–245
18. Yang LH, Liu FC, Han EH (2005) Effects of P/B on the properties of anticorrosive coatings with different particle size. *Prog Org Coat* 53:91–98
19. Chang KCL, Hui FL, Chang YK, Tai HH, Hsin HH, Sheng CY, Jui MY, Jen CY, Yuan H (2008) Effect of amino-modified silica nanoparticles on the corrosion protection properties of epoxy resin-silica hybrid materials. *J Nanosci Nanotechnol* 6:3040–3049
20. Pebere N, Picaud T, Duprat M, Dabosi F (1989) Evaluation of corrosion performance of coated steel by the impedance technique. *Corros Sci* 29:1073–11086
21. Nishimura T (2009) Corrosion resistance of molybdenum containing titanium alloy for overpack in simulating underground environment. *J Nuclear Mater* 385:495–503
22. Benedetti AV, Sumodjo PTA, Nobe K, Cabot PL, Proud WG (1995) Electrochemical studies of copper, copper-aluminium and copper aluminium-silver alloys: impedance results in 0.5 M NaCl. *Electrochim Acta* 40:2657–2668
23. Kouloumbi N, Tsangaris GK, Skordos A, Kyvelidis S (1996) Evaluation of the behavior of particulate polymeric coatings in a



- corrosive environment. Influence of the concentration of metal particles. *Prog Org Coat* 28:117–124
24. Bierwagen G, Tallman D, Li J, He L (2003) EIS studies of coated metals in accelerated exposure. *Prog Org Coat* 46:148–157
  25. Abreu CM, Izquierw M, Keddani M, NoVoia XR, Takenouti H (1996) Electrochemical behavior of Zinc-rich epoxy paints in 3% NaCl solution. *Electrochim Acta* 41:240–2415
  26. Deflorian F, Fedrizzi L, Rossi S (1999) Organic coating capacitance measurement by EIS: ideal and actual trends. *Electrochim Acta* 44:4243–4249
  27. Park JH, Lee GD, Ooshige H, Nishikata A, Tsuru T (2003) Monitoring of water uptake in organic coatings under cyclic wet–dry condition. *Corros Sci* 45:1881–1894
  28. Van Westing EPM, Ferrari GM, De Wit JHW (1993) The determination of coating performance with impedance measurements. *Corros Sci* 34:1511–1530
  29. Bidoia ED, Bulhoes LOS, Rocha-Filho RC (1994) Pt/HClO<sub>4</sub> interface CPE: influence of surface roughness and electrolyte concentration. *Electrochim Acta* 39:763–769
  30. Nishimura T (2008) Rust formation and corrosion performance of Si and Al bearing ultrafine grained weathering steel. *Corros Sci* 50:1306–1312
  31. Nishimura T (2010) Electrochemical behavior and structure of rust formed on Si and Al bearing steel after atmospheric exposure. *Corros Sci* 52:3609–3614
  32. Nishimura T, Tahara A, Kodama T (2001) Effect of Al on the corrosion behavior of low alloy steel in wet/dry environment. *Mater Trans* 42:478–483
  33. Schwertmann U (1984) The influence of aluminium on iron oxides. IX. Dissolution of Al-goethites in 6 M HCl. *Clay Min* 19:9–19
  34. Schwertmann U (1991) Solubility and dissolution of iron oxides. *Plant Soil* 130:1–25